On-top description of the effect of excitation on electron correlation with quasiparticles

Mohammad Reza Jangrouei [1], Katarzyna Pernal [1] and Oleg V. Gritsenko [1,2,*]
[1] *Institute of Physics, Lodz University of Technology, PL-90-924 Lodz, Poland*
[2] *Section Theoretical Chemistry, VU University, NL-1081 HV Amsterdam, The Netherlands*

(Received 7 May 2021; accepted 21 July 2021; published 4 August 2021)

A spectrum of Δ-correlon quasiparticles is proposed to describe the excitation effect on electron correlation. The proposed quasiparticle description is based on the comparison of the pair-correlation functions of the excited and ground states at the special coalescence points of the configurational space. The complex form of the Δ-correlon wave function allows us to naturally separate regions with the excitation suppression of correlation (ESC Δ-correlon), where correlation is stronger in the ground state, from those with the excitation enhancement of correlation (EEC Δ-correlon), where correlation is stronger in the excited state. The proposed Δ-correlon approach is applied to characterize the important single excitations with the competition of "anticorrelation squeezing" and "enhanced-correlation spreading" of the two-electron distribution. The former feature characterizes single valence excitations of the ionic nature and this leads to the prevailing of the ESC effect in this type of excitations. In turn, the enhanced-correlation spreading characterizes single Rydberg excitations, which leads to the prevailing of the EEC effect in this type of excitations. The proposed Δ-correlon quasiparticles are studied both analytically and numerically. The analytical expressions for the on-top correlation functions are obtained with the two-determinantal two-electron model of the active site of an excitation. The two-dimensional contour plots of the ESC and EEC Δ-correlons obtained for the lowest vertical valence ionic and Rydberg excitations in the prototype molecules H_2, N_2, and C_2H_4 from the highly correlated wave functions confirm, in general, the trends in the relative correlation strength deduced from the model.

DOI: 10.1103/PhysRevA.104.022804

I. INTRODUCTION

One of the important goals of conceptual many-electron theory is a systematic description of trends in electron correlation in various types of many-electron states. In theoretical spectroscopy this goal can be reformulated as a comparative description of electron correlation in different types of excited states. Such a description would provide yet another criterion for a meaningful systematization of, otherwise, a veritable "zoo" of molecular electronic excitations.

In our previous work [1] we proposed to employ a type of the quasiparticles, the correlons, as kinematic descriptors of a local effect of electron correlation in individual many-electron states. The term "kinematic" means that a descriptor does not contain the particle interaction or external potential operators, being solely constructed in terms of the generic wave function and the corresponding reduced quantities, such as the reduced density matrices (RDMs). In this paper the differential correlons, Δ-correlons, are proposed to describe the excitation effect on electron correlation. Compared to the correlons of Ref. [1], they accumulate the information from both ground and excited states, thus introducing the important comparative aspects of the excitation description (see below).

In general, quasiparticles offer an efficient conceptual kinematic approach to describe the distributions of electrons and holes in many-electron systems. For excited states a canonical example is the description of the excitation effect on the one-electron quantity, the electron density $\rho(\boldsymbol{r})$, with the exciton quasiparticles [2]. A change of the density $\Delta\rho^P(\boldsymbol{r}_1)$ due to a single-electron excitation

$$\Delta\rho^P(\boldsymbol{r}_1) = \rho^P(\boldsymbol{r}_1) - \rho^0(\boldsymbol{r}_1) = N\int\cdots\int |\Psi_N^P(\boldsymbol{x}_1,\ldots,\boldsymbol{x}_N)|^2 \times d\sigma_1\cdots d\sigma_N d\boldsymbol{r}_2\cdots d\boldsymbol{r}_N - N\int\cdots\int \times |\Psi_N^0(\boldsymbol{x}_1,\ldots,\boldsymbol{x}_N)|^2 d\sigma_1\cdots d\sigma_N d\boldsymbol{r}_2\cdots d\boldsymbol{r}_N \quad (1)$$

is represented as the density $\rho^P_{\rm exc}(\boldsymbol{r}_1)$ of the zero-charge exciton quasiparticle

$$\Delta\rho^P(\boldsymbol{r}_1) = \rho^P_{\rm exc}(\boldsymbol{r}_1) = \rho^P_p(\boldsymbol{r}_1) + \rho^P_h(\boldsymbol{r}_1). \quad (2)$$

In Eq. (1) Ψ_N^0 and Ψ_N^P are the N-electron ground- and excited-state ($P > 0$) wave functions, with $\boldsymbol{x}_i = \{\boldsymbol{r}_i, \sigma_i\}$ being the combination of individual spatial $\boldsymbol{r}_i$ and spin σ_i electron coordinates. In Eq. (2) $\rho^P_p(\boldsymbol{r}_1)$ and $\rho^P_h(\boldsymbol{r}_1)$ are the "particle" and "hole" densities. Depending on the type of the system, excitons can greatly differ in a degree of their localization. Atomic and molecular excitons are the short-range limit of the Frenkel excitons [3], while the long-range Wannier-Mott excitons describe excitations in semiconductors [4].

In our development we use the full advantage of the quasiparticle approach to provide the effective one-particle description of many-electron effects. This description is given by considering electron correlation at special coalescence

*o.gritsenko@vu.nl

points of the many-electron configurational space, in which the coordinates of two electrons coincide, $\boldsymbol{r}_1 = \boldsymbol{r}_2 = \boldsymbol{r}$. At these points, electron correlation is represented with the on-top pair density $\Pi^P(\boldsymbol{r})$, which is defined as the pair density function $\rho_2^P(\boldsymbol{r}_1, \boldsymbol{r}_2)$ evaluated at $\boldsymbol{r}$ [5],

$$\Pi^P(\boldsymbol{r}) = \rho_2^P(\boldsymbol{r}, \boldsymbol{r}) = N(N-1) \int \cdots \int |\Psi_N^P(\boldsymbol{x}_1, \ldots, \boldsymbol{x}_n)|^2 \times d\sigma_1 \cdots d\sigma_N d\boldsymbol{r}_3 \cdots d\boldsymbol{r}_N|_{\boldsymbol{r}_1=\boldsymbol{r}_2=\boldsymbol{r}}. \quad (3)$$

Importantly, the coalescence points appear to be representative for the description of both main modes of electron correlation, which are dynamic and nondynamic correlation. Because of this, the on-top function $\Pi^P(\boldsymbol{r})$ is employed to connect wave function theory (WFT) [6] and density functional theory (DFT) [7–10] in the ongoing development of efficient combined methods of the electronic structure calculations [11–17]. In particular, left-right nondynamic correlation of electrons of a two-electron bond [18] is reflected in relatively low values of $\Pi^P(\boldsymbol{r})$ for the coalescence points $\boldsymbol{r}$ in the corresponding bonding region. This feature allows one to employ $\Pi^P(\boldsymbol{r})$ in the description of instantaneous spin polarization of electrons of dissociating bonds due to their nondynamic (strong) correlation [12]. Naturally the coalescence points are also representative for the description of short-range dynamic correlation. Because of this, the on-top function $\Pi^P(\boldsymbol{r})$ is used to model pair-correlation functions describing this effect [15,19,20] .

In our recent WFT + DFT development both above mentioned features are utilized to describe finer correlation effects, such as the local suppression of dynamic correlation (SDC) with nondynamic correlation as well as enhancement of dynamic correlation (EDC) in the cases of "squeezing" of the two-electron distribution at the initial level of a few-determinantal wave function [17]. The modeling of the SDC and EDC effects became the basis of the recent WFT-DFT method CASΠDFT [14,16,17,21–24]. It efficiently combines the WFT complete active space (CAS) method with the DFT correlation energy functional of Lee, Yang, and Parr (LYP) [25] corrected for SDC and EDC.

In this paper the on-top quasiparticle description is applied to describe the excitation effect on electron correlation for the important lowest single $\psi \rightarrow \phi$ excitations of singlet symmetry, where ψ is the bonding molecular orbital (MO), which is occupied in the reference Slater determinant representing the ground state, while ϕ is one of the lowest virtual MOs. The nature of the latter MO determines the type of the $\psi \rightarrow \phi$ excitation. If ϕ is the antibonding MO corresponding to the bonding MO ψ, then we have a valence excitation of the ionic nature [17,26,27]. A promotion to a delocalized Rydberg MO ϕ determines the Rydberg character of the corresponding excitation. Below, it will be shown that qualitative trends of electron correlation in these types of excitations can be understood already in the minimal two-determinantal two-electron representation of the active wave function Ψ_e^{act},

$$\Psi_e^{\text{act}} = \tfrac{1}{2}[\psi(\boldsymbol{r}_1)\phi(\boldsymbol{r}_2) + \phi(\boldsymbol{r}_1)\psi(\boldsymbol{r}_2)][\alpha(1)\beta(2) - \beta(1)\alpha(2)], \quad (4)$$

a part of the total excited state Ψ_N^P,

$$\Psi_N^P \approx \mathcal{A}(\Psi_{N-2}^{\text{core}} \Psi_e^{\text{act}}), \quad (5)$$

In Eq. (4) α and β are the spin functions, i.e., functions describing the z component of electron spin, corresponding, respectively to $s_z = 1/2$ and $s_z = -1/2$. In Eq. (5) Ψ_{N-2}^{core} is the "core" part of Ψ_N^P, which is not involved in the excitation, while $\mathcal{A}$ is the antisymmetrization and normalization operator. The present inclusion of the Rydberg type excitations and the analytic study of the excitation effect on electron correlation constitute an important advance compared to our previous work [1].

In Sec. II of this paper, a spectrum of Δ-correlon quasiparticles is proposed to describe a local excitation effect on the electron Coulomb correlation for various excited states. A wave function of a delta-correlon is constructed from the difference between the excited- and ground-state pair-correlation functions. In Sec. III the trends of electron correlation in valence ionic and Rydberg excitations are analyzed with the two-determinantal two-electron model. Section IV presents Δ-correlons constructed numerically for the valence ionic and Rydberg excitations in prototype molecules H_2, N_2, and C_2H_4. In Sec. V general trends in electron correlation in the considered types of excitations are discussed and the conclusions are drawn.

II. Δ-CORRELON QUASIPARTICLES

In this section a spectrum of Δ-correlon quasiparticles is proposed based on the on-top approach, which has been characterized in Sec. I. Note, first of all, that this approach naturally separates out the leading effect of the Coulomb correlation of electrons with the opposite spins. Indeed, due to the antisymmetry of the fermionic wave function, the same-spin component of the on-top pair density is zero, $\Pi^{P(\uparrow\uparrow)}(\boldsymbol{r}) = 0$, so $\Pi^P(\boldsymbol{r})$ is identically equal to its opposite-spin component $\Pi^{P(\uparrow\downarrow)}(\boldsymbol{r})$,

$$\Pi^P(\boldsymbol{r}) \equiv \Pi^{P(\uparrow\downarrow)}(\boldsymbol{r}). \quad (6)$$

Then the natural reference valid for all states is the uncorrelated counterpart $\Pi_u^{P(\uparrow\downarrow)}(\boldsymbol{r})$ of $\Pi^{P(\uparrow\downarrow)}(\boldsymbol{r})$,

$$\Pi_u^{P(\uparrow\downarrow)}(\boldsymbol{r}) = \tfrac{1}{2}[\rho^P(\boldsymbol{r})]^2, \quad (7)$$

a half of the square of the electron density $\rho^P(\boldsymbol{r})$. In $\Pi_u^{P(\uparrow\downarrow)}(\boldsymbol{r})$ correlation only implicitly affects $\rho^P(\boldsymbol{r})$. Thus, the ratio of $\Pi^{P(\uparrow\downarrow)}(\boldsymbol{r})$ to $\Pi_u^{P(\uparrow\downarrow)}(\boldsymbol{r})$, the on-top pair-correlation function $X^P(\boldsymbol{r})$,

$$X^P(\boldsymbol{r}) = \frac{\Pi^{P(\uparrow\downarrow)}(\boldsymbol{r})}{\Pi_u^{P(\uparrow\downarrow)}(\boldsymbol{r})} = \frac{2\Pi^P(\boldsymbol{r})}{[\rho^P(\boldsymbol{r})]^2}, \quad (8)$$

gives the explicit effect of electron Coulomb correlation. Typically it is the reduction of the pair density in the vicinity of the coalescence point compared to its uncorrelated counterpart $[\rho^P(\boldsymbol{r})]^2/2$, due to which $X^P(\boldsymbol{r})$ becomes a fraction $X^P(\boldsymbol{r}) < 1$. In addition, excited states of the ionic nature treated with the restricted account of, predominantly, nondynamic correlation are characterized with regions, in which the ratio Eq. (8) exceeds the value 1, $X^P(\boldsymbol{r}) > 1$, due to the instantaneous squeezing of electrons in the configurational space [14,17,24].

In our previous work [1], based on the correlation amplitude $c^P(\boldsymbol{r})$, the square root of $X^P(\boldsymbol{r}) - 1$,

$$c^P(\boldsymbol{r}) = \sqrt{X^P(\boldsymbol{r}) - 1}, \tag{9}$$

the correlon quasiparticles were introduced to describe the local correlation effect in the individual states Ψ_N^P. Our present goal is the comparative description of electron correlation in the excited and ground states, in order to analyze the excitation effect on correlation. To this end, in an analogy with the exciton approach of Eqs. (1) and (2), we consider the difference $\Delta X^P(\boldsymbol{r})$ between the excited- and ground-state on-top pair-correlation functions

$$\Delta X^P(\boldsymbol{r}) = X^P(\boldsymbol{r}) - X^0(\boldsymbol{r}). \tag{10}$$

To convert this difference to the quasiparticle picture, we introduce the differential correlation amplitude $c_\Delta^P(\boldsymbol{r})$, the square root of $\Delta X^P(\boldsymbol{r})$,

$$c_\Delta^P(\boldsymbol{r}) = \sqrt{\Delta X^P(\boldsymbol{r})}. \tag{11}$$

The amplitude $c_\Delta^P(\boldsymbol{r})$ naturally separates the spatial regions, in which the on-top pair-correlation function is smaller in the ground state $[\Delta X^P(\boldsymbol{r}) > 0]$, from those in which it is smaller in the excited state $[\Delta X^P(\boldsymbol{r}) < 0]$. Indeed, the former regions are represented with the nonvanishing real part of the amplitude $\mathrm{Re}[c_\Delta^P(\boldsymbol{r})]$, while the latter regions are represented with its nonvanishing imaginary part $\mathrm{Im}[c_\Delta^P(\boldsymbol{r})]$. Based on the definition Eq. (8) of the pair-correlation function, one can consider the regions of location of $\mathrm{Re}[c_\Delta^P(\boldsymbol{r})]$ as those with the excitation suppression of correlation (ESC), in which excitation results in a weaker correlation strength at the coalescence points. The regions of location of $\mathrm{Im}[c_\Delta^P(\boldsymbol{r})]$ can be considered in turn as those with the excitation enhancement of correlation (EEC), in which excitation results in a higher correlation strength.

By its definition, the differential correlation amplitude $c_\Delta^P(\boldsymbol{r})$ does not necessarily vanish in the energetically unimportant regions of low electron density $\rho^P(\boldsymbol{r})$. Because of this, it is not normalizable by itself, so it cannot be directly employed as a quasiparticle wave function. Then, in order to turn it into a normalizable function, which would describe electron correlation in the important spatial regions, we apply the density cutoff to the on-top pair-correlation functions

$$\tilde{X}^P(\boldsymbol{r}) = X^P(\boldsymbol{r})\frac{\rho^0(\boldsymbol{r})}{a + \rho^0(\boldsymbol{r})}. \tag{12}$$

With a sufficiently small parameter a of the cut-off Padé approximant in Eq. (12), the function $\tilde{X}^P(\boldsymbol{r})$ is approximately equal to the original function $X^P(\boldsymbol{r})$, $\tilde{X}^P(\boldsymbol{r}) \approx X^P(\boldsymbol{r})$ in the energetically important regions of typical atomic and molecular energy densities. On the other hand, $\tilde{X}^0(\boldsymbol{r})$, $\tilde{X}^P(\boldsymbol{r})$, and their difference $\Delta\tilde{X}^P(\boldsymbol{r})$,

$$\Delta\tilde{X}^P(\boldsymbol{r}) = \tilde{X}^P(\boldsymbol{r}) - \tilde{X}^0(\boldsymbol{r}) = [X^P(\boldsymbol{r}) - X^0(\boldsymbol{r})]\frac{\rho^0(\boldsymbol{r})}{a + \rho^0(\boldsymbol{r})}, \tag{13}$$

all decay exponentially with $\rho^0(\boldsymbol{r})$ in the regions of low density. The use of the common cutoff for all states, which employs the ground-state density $\rho^0(\boldsymbol{r})$, would preserve the most important information, the local ESC or the EEC character of the differential on-top pair-correlation $\Delta X^P(\boldsymbol{r})$.

With this cutoff, we propose a quasiparticle description of excitation effect on electron correlation. To this end, we introduce for each excited state $\Psi_N^P(\boldsymbol{x}_1, \ldots, \boldsymbol{x}_N)$ the corresponding Δ-correlon quasiparticle represented with the one-electron wave function $\psi_{\Delta c}^P(\boldsymbol{r})$,

$$\psi_{\Delta c}^P(\boldsymbol{r}) = \frac{1}{\sqrt{N_{\Delta c}^P}}\sqrt{\tilde{X}^P(\boldsymbol{r}) - \tilde{X}^0(\boldsymbol{r})}, \tag{14}$$

where $N_{\Delta c}^P$ is its normalization

$$N_{\Delta c}^P = \int |\tilde{X}^P(\boldsymbol{r}) - \tilde{X}^0(\boldsymbol{r})| d\boldsymbol{r}. \tag{15}$$

Just as the differential correlation amplitude $c_\Delta^P(\boldsymbol{r})$ of Eq. (11), the Δ-correlon wave function $\psi_{\Delta c}^P(\boldsymbol{r})$ of Eq. (14) provides a natural separation of regions, in which the local correlation is either stronger or weaker in the excited state. Specifically, the real part of the Δ-correlon wave function $\mathrm{Re}[\psi_{\Delta c}^P(\boldsymbol{r})]$ represents ESC. Then, this part can be called an ESC Δ-correlon,

$$\mathrm{Re}[\psi_{\Delta c}^P(\boldsymbol{r})] \equiv \psi_{\Delta c}^{P(\mathrm{ESC})}(\boldsymbol{r}), \tag{16}$$

a kinematic local index describing the magnitude and location of ESC. In turn, the imaginary part $\mathrm{Im}[\psi_{\Delta c}^P(\boldsymbol{r})]$ represents EEC. So this part can be called an EEC Δ-correlon,

$$\mathrm{Im}[\psi_{\Delta c}^P(\boldsymbol{r})] \equiv \psi_{\Delta c}^{P(\mathrm{EEC})}(\boldsymbol{r}). \tag{17}$$

With the overall normalization as in Eq. (15), the amplitudes of the Δ-correlons Eqs. (16) and (17) show a relative prominence of the corresponding ESC and EEC effects.

III. ANALYTICAL EXPRESSIONS FOR Δ-CORRELONS IN A TWO-DETERMINANTAL TWO-ELECTRON MODEL

The expressions for the Δ-correlons derived in this section within the two-determinantal two-electron active part model allow one to compare the effective correlation in the singly excited state Ψ_e^{act} of Eq. (4) with the canonical electron correlation in the partially doubly excited ground state Ψ_g^{act},

$$\Psi_g^{\mathrm{act}} = \frac{1}{\sqrt{2}}[c_1\psi(\boldsymbol{r}_1)\psi(\boldsymbol{r}_2) - c_2\phi(\boldsymbol{r}_1)\phi(\boldsymbol{r}_2)][\alpha(1)\beta(2) - \beta(1)\alpha(2)]. \tag{18}$$

The optimization of Eq. (18) according to the variational principle produces the minus sign between two spatial terms with the positive coefficients c_1 and c_2, and the normalization condition for the wave function imposes that $c_1^2 + c_2^2 = 1$. In Eq. (18) $\psi(\boldsymbol{r})$ is the bonding MO,

$$\psi(\boldsymbol{r}) = \frac{1}{\sqrt{2}}[\chi_a(\boldsymbol{r}) + \chi_b(\boldsymbol{r})], \tag{19}$$

while orthogonal $\phi(\boldsymbol{r})$ orbital is the antibonding MO,

$$\phi(\boldsymbol{r}) = \frac{1}{\sqrt{2}}[\chi_a(\boldsymbol{r}) - \chi_b(\boldsymbol{r})]. \tag{20}$$

In Eqs. (19) and (20), $\chi_a(\boldsymbol{r})$ and $\chi_b(\boldsymbol{r})$ are orthonormal atomiclike orbitals (AOs) localized on atoms A and B, respectively, of a two-center two-electron bond A–B.

The magnitude of the on-top functions $\Pi_e^{\rm act}(\boldsymbol{r})$ and $X_e^{\rm act}(\boldsymbol{r})$, pertaining to the wave function in Eq. (18), is determined by the competition of two opposing effects of "anticorrelation squeezing" and "enhanced-correlation spreading" of the two-electron distribution due to a single excitation. Anticorrelation squeezing, which tends to higher values of the on-top functions, stems from the plus sign in the spatial part of the generic wave function $\Psi_e^{\rm act}$ of Eq. (4), which is opposite to the minus sign in the genuinely correlated ground state $\Psi_g^{\rm act}$ of Eq. (18). This plus sign produces a relatively high numerical prefactor 4 of the corresponding on-top pair density $\Pi_e^{\rm act}(\boldsymbol{r})$,

$$\Pi_e^{\rm act}(\boldsymbol{r}) = 4\psi(\boldsymbol{r})^2\phi(\boldsymbol{r})^2. \tag{21}$$

Enhanced-correlation spreading, which tends to lower values of the on-top functions, stems from the degree or the region of localization of the orbital $\phi(\boldsymbol{r})$, which accommodates the excited electron. Specifically, as was already mentioned in Sec. I, Rydberg excitations are characterized by the diffuse character of the MO $\phi(\boldsymbol{r})$. This causes relatively low values of the differential overlap of the MO squares $\psi(\boldsymbol{r})^2\phi(\boldsymbol{r})^2$, which counter the high numerical prefactor 4 in Eq. (21).

After this general characterization of single excitations, we turn to valence excitations of the ionic nature. In this case, $\Psi_e^{\rm act}$ of Eq. (4) consists of the MOs given in Eqs. (19) and (20), with the localized AOs $\chi_a(\boldsymbol{r})$, $\chi_b(\boldsymbol{r})$ as for the ground state. Thus, valence ionic excitations are characterized just with the above mentioned anticorrelation squeezing. Then, in the energetically important regions in the vicinity of the nuclei the on-top pair-correlation function $X_e^{\rm act}(\boldsymbol{r})$,

$$X_e^{\rm act}(\boldsymbol{r}) = \frac{2\chi_a(\boldsymbol{r})^4 + 2\chi_b(\boldsymbol{r})^4 - 4\chi_a(\boldsymbol{r})^2\chi_b(\boldsymbol{r})^2}{\chi_a(\boldsymbol{r})^4 + \chi_b(\boldsymbol{r})^4 + 2\chi_a(\boldsymbol{r})^2\chi_b(\boldsymbol{r})^2} \tag{22}$$

attains relatively high values $X_e^{\rm act}(\boldsymbol{r}) > 1$, for the region around the nucleus A, where $\chi_b(\boldsymbol{r})^2 \ll \chi_a(\boldsymbol{r})^2$. This can be shown with the expansion of $X_e^{\rm act}(\boldsymbol{r})$ with respect to the ratio $\chi_b(\boldsymbol{r})^2/\chi_a(\boldsymbol{r})^2$,

$$X_e^{\rm act}(\boldsymbol{r})|_{\chi_b(\boldsymbol{r})^2/\chi_a(\boldsymbol{r})^2<<1} \approx 2 - 8\frac{\chi_b(\boldsymbol{r})^2}{\chi_a(\boldsymbol{r})^2} > 1. \tag{23}$$

The proposed Δ-correlon approach compares $X_e^{\rm act}(\boldsymbol{r})$ of Eq. (22) with the corresponding ground-state function $X_g^{\rm act}(\boldsymbol{r})$, defined in analogy to Eq. (8) by using the on-top pair density $\Pi_g^{\rm act}(\boldsymbol{r})$ obtained from Eq. (18),

$$\Pi_g^{\rm act}(\boldsymbol{r}) = \tfrac{1}{2}\{(c_1 - c_2)[\chi_a(\boldsymbol{r})^2 + \chi_b(\boldsymbol{r})^2] + 2(c_1 + c_2)\chi_a(\boldsymbol{r})\chi_b(\boldsymbol{r})\}^2, \tag{24}$$

and the density $\rho_g^{\rm act}(\boldsymbol{r})$,

$$\rho_g^{\rm act}(\boldsymbol{r}) = \chi_a(\boldsymbol{r})^2 + \chi_b(\boldsymbol{r})^2 + 2(c_1^2 - c_2^2)\chi_a(\boldsymbol{r})\chi_b(\boldsymbol{r}), \tag{25}$$

which reads

$$X_g^{\rm act}(\boldsymbol{r}) = \frac{\{(c_1 - c_2)[\chi_a(\boldsymbol{r})^2 + \chi_b(\boldsymbol{r})^2] + 2(c_1 + c_2)\chi_a(\boldsymbol{r})\chi_b(\boldsymbol{r})\}^2}{[\chi_a(\boldsymbol{r})^2 + \chi_b(\boldsymbol{r})^2 + 2(c_1^2 - c_2^2)\chi_a(\boldsymbol{r})\chi_b(\boldsymbol{r})]^2}. \tag{26}$$

At variance with $X_e^{\rm act}(\boldsymbol{r})$ of Eq. (23), the on-top function $X_g^{\rm act}(\boldsymbol{r})$ of Eq. (26) is relatively low, $X_g^{\rm act}(\boldsymbol{r}) < 1$ in the vicinity of the nuclei. This can be also shown with the expansion of $X_g^{\rm act}(\boldsymbol{r})$ with respect to the ratio $\chi_b(\boldsymbol{r})^2/\chi_a(\boldsymbol{r})^2$. Retaining the two leading terms in this expansion yields

$$X_g^{\rm act}(\boldsymbol{r})|_{\chi_b(\boldsymbol{r})^2/\chi_a(\boldsymbol{r})^2\ll 1} \approx \frac{\rho_g^{\rm act}(\boldsymbol{r})^2 - 2c_1c_2\chi_a(\boldsymbol{r})^4}{\rho_g^{\rm act}(\boldsymbol{r})^2} < 1. \tag{27}$$

Finally, from the comparison of Eq. (23) with Eq. (27) follows, that their difference $\Delta X^{\rm act}(\boldsymbol{r})$ is positive in the vicinity of the nuclei. This means, that for valence excitations of the ionic nature the ESC correlon Eq. (16) is located in this region. Bearing in mind the energetical importance of this region, one can conclude that the strength of correlation in the active part of the wave function varies in the order

$$\text{valence ionic excitations} < \text{ground state}.$$

Next, we turn to Rydberg single excitations. In this case, as was already mentioned above, the diffuse nature of the terminal MO $\phi(\boldsymbol{r})$, leads to reduction of $\Pi_e^{\rm act}(\boldsymbol{r})$ given in Eq. (21) as well as of the on-top pair correlation function $X_e^{\rm act}(\boldsymbol{r})$,

$$X_e^{\rm act}(\boldsymbol{r}) = \frac{8\psi(\boldsymbol{r})^2\phi(\boldsymbol{r})^2}{\psi(\boldsymbol{r})^4 + 2\psi(\boldsymbol{r})^2\phi(\boldsymbol{r})^2 + \phi(\boldsymbol{r})^4}. \tag{28}$$

Furthermore, the denominator of the formula Eq. (28) for $X_e^{\rm act}(\boldsymbol{r})$ contains, besides the small term $\psi(\boldsymbol{r})^2\phi(\boldsymbol{r})^2$, also a relatively large term $\psi(\boldsymbol{r})^4$ with the localized MO $\psi(\boldsymbol{r})$. Consequently, one can expect that, contrary to valence ionic excitations, $X_e^{\rm act}(\boldsymbol{r})$ can attain for Rydberg excitations rather low values $X_e^{\rm act}(\boldsymbol{r}) < 1$.

Comparing the trends established above, one can conclude that the strength of effective correlation in active part varies in the order

$$\text{valence ionic excitations} < \text{ground state} < \text{Rydberg excitations}.$$

The qualitative trends established in this section for the two-determinantal two-electron model will serve as a guiding line in the analysis of the spatial distribution of the ESC and EEC Δ-correlons obtained in the next section.

IV. Δ-CORRELONS FOR VALENCE IONIC AND RYDBERG EXCITATIONS IN PROTOTYPE MOLECULES

In this section the spatial behavior is analyzed of the Δ-correlons obtained for the prototype molecules H_2, N_2, and C_2H_4 described at a rather highly correlated level with the self-consistent field CAS method CASSCF(n, m), which includes all possible distributions of n electrons in the active orbital space of m orbitals of the reference determinants. Vertically excited states are studied and the assumed ground state geometries for the molecules read: H_2: $R_{H_2} = 1.40$ bohr, N_2: $R_{N_2} = 2.08$ bohr, C_2H_4: $R_{CC} = 2.53$ bohr, $R_{CH} = 2.05$ bohr,

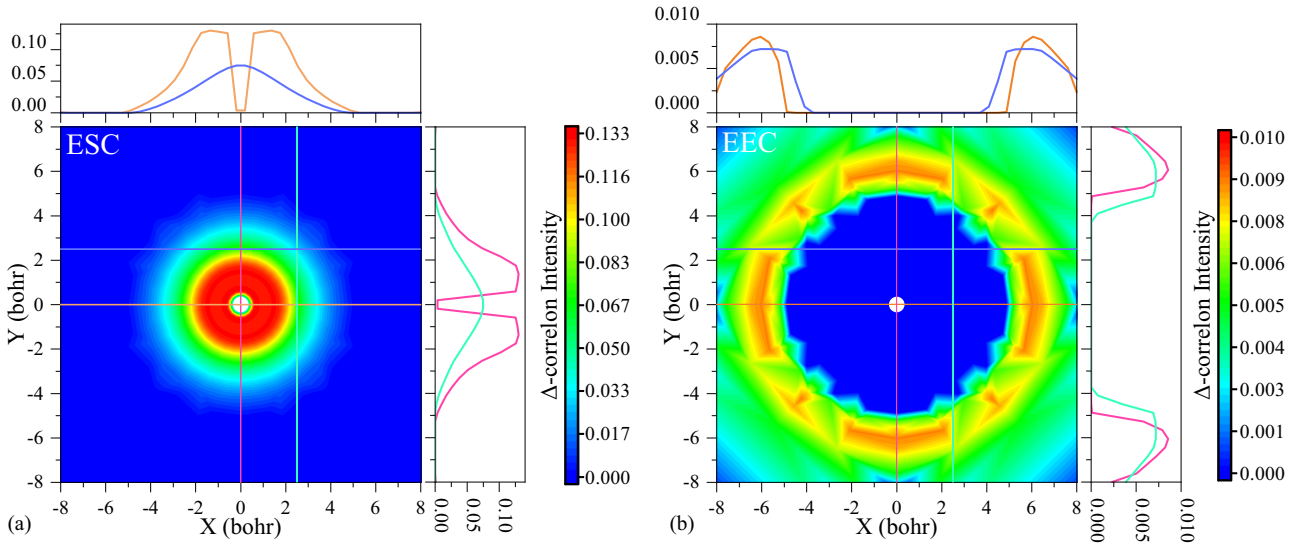

FIG. 1. Plots of ESC (left panel) and EEC (right panel) Δ-correlon functions, cf. Eqs. (16) and (17), respectively, for the $\Sigma_u^-(\pi \to \pi^*)$ state of N_2. The XY plane is perpendicular to the axis of the molecule and includes the position of one of the N nuclei located in the center.

$\angle_{HCH} = 116.6$ deg. The comparative behavior of the ESC and EEC Δ-correlons is described as their "competition" for the energetically important regions in the vicinity of the nuclei.

In all calculations of Δ-correlons functions, the value of the parameter a of the cut-off Padé function in Eq. (12) was set to 0.01 in agreement with our previous work [1].

A. Valence ionic excitations

First, we consider Δ-correlons obtained for the lowest singly excited valence states of the ionic nature. The states considered in this subsection are the $\Sigma_u^-(\pi \to \pi^*)$ states of N_2 and C_2H_4 as well as the $\Pi_g(\sigma \to \pi^*)$ state of C_2H_4. In the case of N_2 the generic excited- and ground-state wave functions are obtained with the CAS(6,14) in the augmented correlation-consistent valence double-zeta (plus polarization functions) aug-cc-pVDZ basis [28,29], while in the case of the C_2H_4 the wave functions are obtained with the CAS(10,14) in the aug-cc-pVTZ basis.

Figures 1–3 display the two-dimensional (2D) contour plots of the Δ-correlons for the above mentioned states in the XY plane perpendicular to the A–A bond axis, which passes through one of the A nuclei depicted with the circle in the center of the plot. For C_2H_4 two small circles on the Y axis of Figs. 2 and 3 indicate the projections of the H nuclei on the plot plane. The behavior of the ESC and EEC Δ-correlons confirms the predictions of the two-determinantal two-electron model of Sec. III for this type of excitations. Indeed, in all cases the ESC Δ-correlon "wins" an energetically favorable position in the vicinity of the nucleus [see Figs. 1(a)–3(a)]. Its shape clearly reflects the difference [compare Figs. 2(a) and 3(a) with Fig. 1(a)] between the C_2H_4 and N_2 molecules with a single and double π bonds, respectively. Indeed, in the former case the ESC Δ-correlon has a p-AO like shape perpendicular to the molecular plane [see Figs. 2(a) and 3(a)], while in a more symmetrical N_2 case the ESC Δ-correlon forms a circle around the N nucleus [see Fig. 1(a)].

In turn, the EEC Δ-correlon is pushed outwards in all cases and it forms a "halo" around the ESC Δ-correlon, as it can be seen in Figs. 1(b)–3(b). Understandably, the halo shape is most symmetrical in the case of N_2, where it forms a circular ring [see Fig. 1(b)]. In the case of C_2H_4 it has an elliptic ring shape for the Π_g state [see Fig. 3(b)], while for the Σ_u^- state the halo is concentrated, mainly, at two peaks around the Y axis of the molecular plane [see Fig. 2(b)].

Overall, the established behavior of the ESC Δ-correlon indicates that (in the agreement with the prediction in Sec. III) the strength of correlation varies in the order

$$\text{valence ionic excitations} < \text{ground state}.$$

In order to understand this agreement, one can represent the accurate wave function of the singly excited state Ψ_e as a combination of the two determinants extending the active part model plus the rest of possible excitations

$$\Psi_e = c_\psi^\phi(|\Phi_{\text{core}}\psi_\alpha\phi_\beta| + |\Phi_{\text{core}}\phi_\alpha\psi_\beta|) + \cdots, \tag{29}$$

where Φ_{core} is the core configuration of both determinants. Similarly, the extension of the active part model for the accurate ground state wave function Ψ_g reads

$$\Psi_g = c_1|\Phi_{\text{core}}\psi_\alpha\psi_\beta| - c_2|\Phi_{\text{core}}\phi_\alpha\phi_\beta| + \cdots. \tag{30}$$

One can say, that in the case of valence ionic excitations the build-up of the excited state Ψ_e starts with anticorrelation squeezing in the active part of the two-determinantal reference Eq. (29), while that of the ground state Ψ_g starts with the two-determinantal reference in Eq. (30) with the genuine electron correlation. Then, electron correlation included with the rest of excitations reduces the magnitude of the corresponding on-top functions $X_e(\boldsymbol{r})$ and $X_g(\boldsymbol{r})$, so that the former drops below 1. Yet, this does not change their qualitative relation $X_e(\boldsymbol{r}) > X_g(\boldsymbol{r})$ in the vicinity of the nuclei, so that their difference determines the localization of the ESC Δ-correlon in this region.

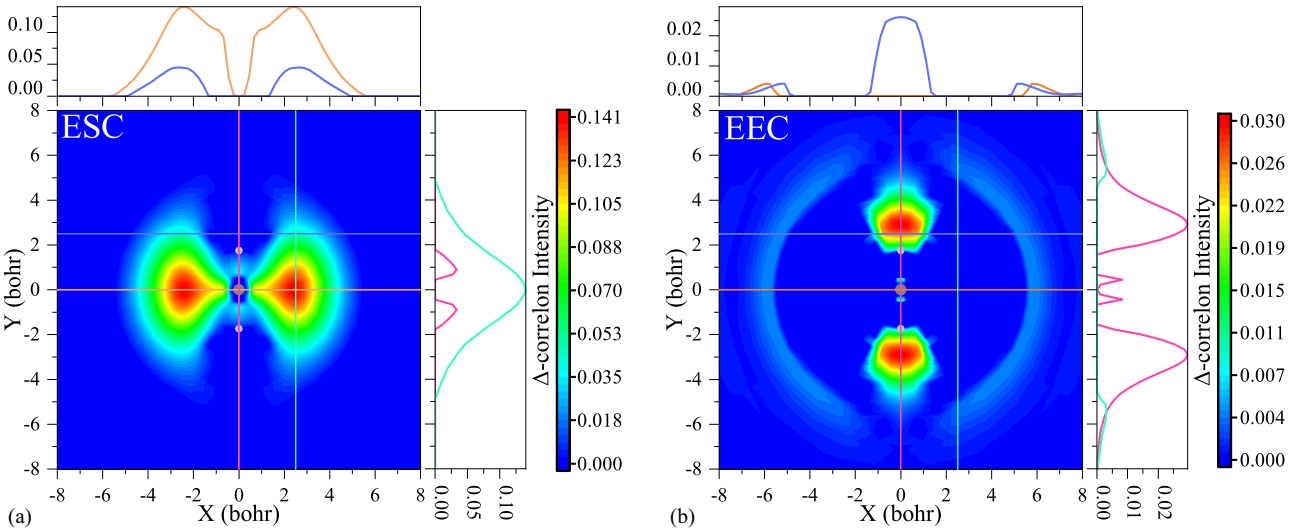

FIG. 2. Plots of ESC (left panel) and EEC (right panel) Δ-correlon functions, cf. Eqs. (16) and (17), respectively, for the $\Sigma_u^-(\pi \rightarrow \pi^*)$ state of C_2H_4. The XY plane is perpendicular to the axis of the molecule and includes the position of one of the C nuclei located in the center.

B. Rydberg excitations

Next, we consider Δ-correlons obtained for Rydberg excitations. The states considered in this subsection is the $\Sigma_g^+(\sigma \rightarrow 2s)$ state of H_2 as well as the $\Pi_u(\pi \rightarrow 3s)$ states of N_2 and C_2H_4. For H_2 and N_2 the generic wave functions are obtained with the CAS(2,32) and CAS(6,19), respectively, in the aug-cc-pVTZ (H_2) or aug-cc-pVDZ (N_2) basis sets [28,29]. In the case of the C_2H_4 the wave function is obtained with CAS(10,14) in the aug-cc-pVTZ basis. The present augmentation of the basis with the additional diffuse functions is a prerequisite for the adequate description of a diffuse electron distribution in the active parts of Rydberg states.

Figures 4–6 display the 2D contour plots of the Δ-correlons for the above mentioned states. At variance with the setting of the 2D plots for C_2H_4 characterized in Sec. IV A, for H_2 the XZ plane of the plot passes through the bond and two small circles on the Z axis indicate the positions of the H nuclei. In agreement with the model of Sec. III, for the considered Rydberg states the behavior of the ESC and EEC Δ-correlons is totally reversed, compared to that for the valence ionic states analyzed above. This time, the EEC Δ-correlon wins in all cases the energetically important regions. Specifically, it occupies both interior and near exterior regions of the H–H bond [see Fig. 4(b)] as well as the regions in the vicinity of the C and N nuclei [see Figs. 5(b) and 6(b)]. In all cases the ESC Δ-correlon is pushed outwards, forming a halo around the EEC Δ-correlon [compare Figs. 4(a)–6(a) with Figs. 4(b)–6(b)]. The halo has a circular ring shape in the case of H_2 [see Fig. 4(a)], while in other two cases it forms two crescent shapes [see Figs. 5(a) and 6(a)]. In the case of N_2 the ESC Δ-correlon crescents form two pockets in the distribution of the EEC Δ-correlon, which occupies also the outermost region [see Fig. 6(b)].

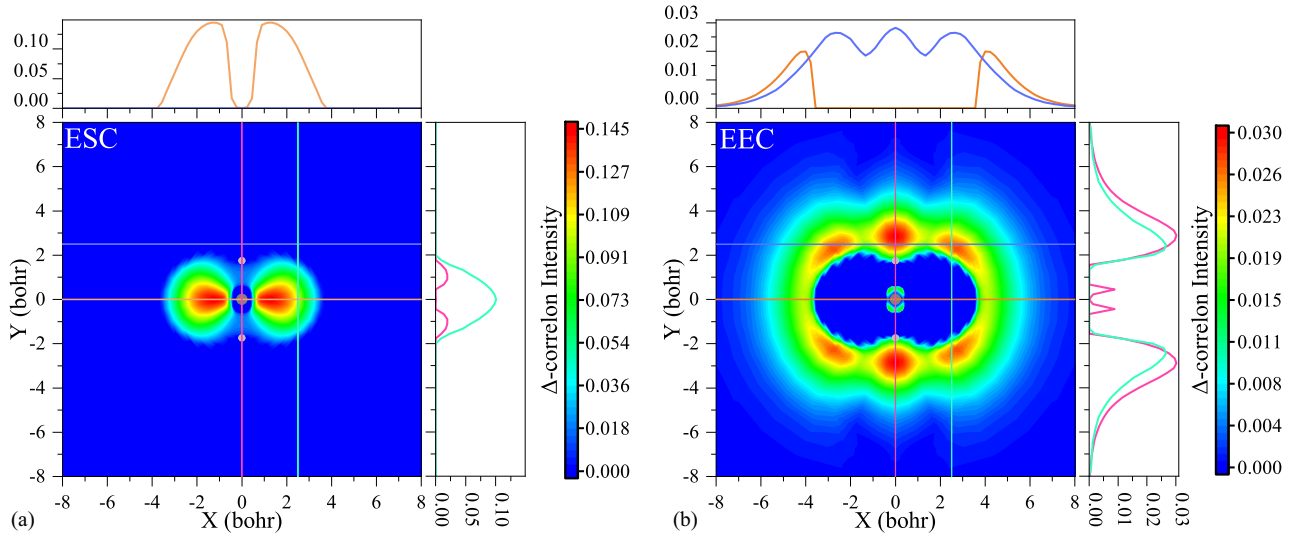

FIG. 3. Plots of ESC (left panel) and EEC (right panel) Δ-correlon functions, cf. Eqs. (16) and (17), respectively, for the $\Pi_g(\sigma \rightarrow \pi^*)$ state of C_2H_4. The XY plane is perpendicular to the axis of the molecule and includes the position of one of the C nuclei located in the center.

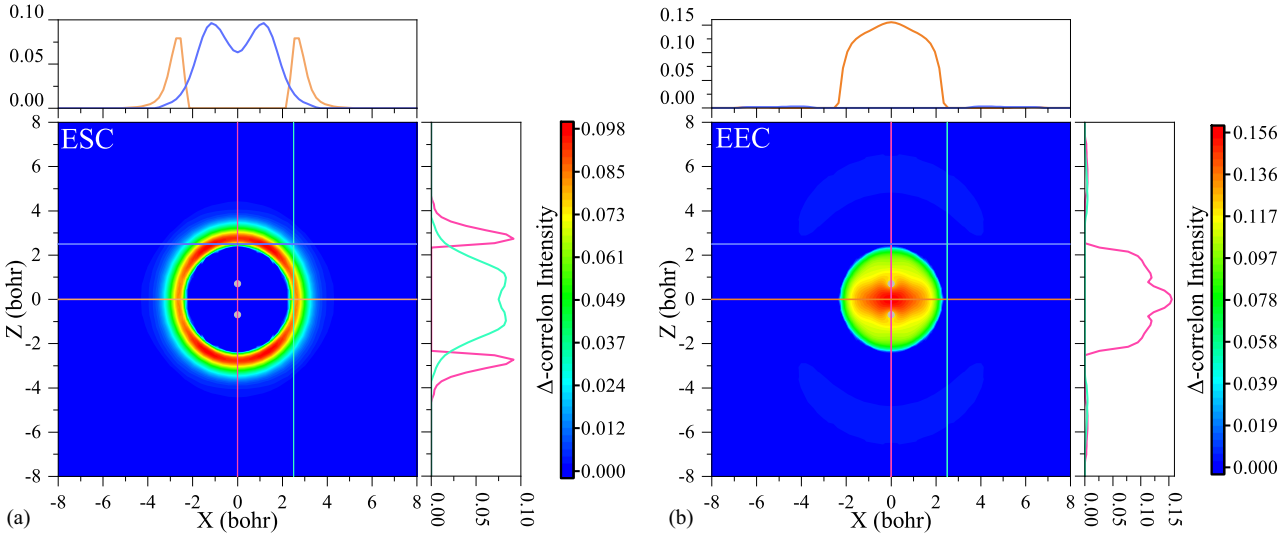

FIG. 4. Plots of ESC (left panel) and EEC (right panel) Δ-correlon functions, cf. Eqs. (16) and (17), respectively, for the $\Sigma_g^+(\sigma \to 2s)$ state of H_2. The Z axis passes through both H nuclei.

Overall, the established behavior of the EEC Δ-correlon shows that (again, in the agreement with the prediction in Sec. III) the strength of correlation varies in the order

ground state < Rydberg excitations.

The established trend can be also rationalized with the expressions Eqs. (29) and (30) for the excited Ψ_e and ground Ψ_g state wave functions. This time, the active part of the two-determinantal reference Eq. (29) embodies enhanced-correlation spreading, which leads to stronger correlation than the genuine one in the ground-state two-determinantal reference in Eq. (30). Again, the additional correlation coming from the rest of the excitations lowers both on-top functions $X_e(\boldsymbol{r})$ and $X_g(\boldsymbol{r})$. Yet, their relation $X_e(\boldsymbol{r}) < X_g(\boldsymbol{r})$ qualitatively holds in the vicinity of the nuclei, so that their difference determines the localization of the EEC Δ-correlon in this region.

Finally, two trends established above can be combined in the overall trend in the local strength of (effective) electron correlation, which increases in the series

valence ionic excitations < ground state < Rydberg excitations.

C. Special cases with a more even competition of the ESC and EEC Δ-correlons

Surprisingly, the canonical $\sigma \to \sigma^*$ valence ionic excitation in H_2 represents, to some extent, a reversal of the trend established for other excitations of this type in Sec. IV A. Figure 7 displays the 2D plots of the Δ-correlons of the

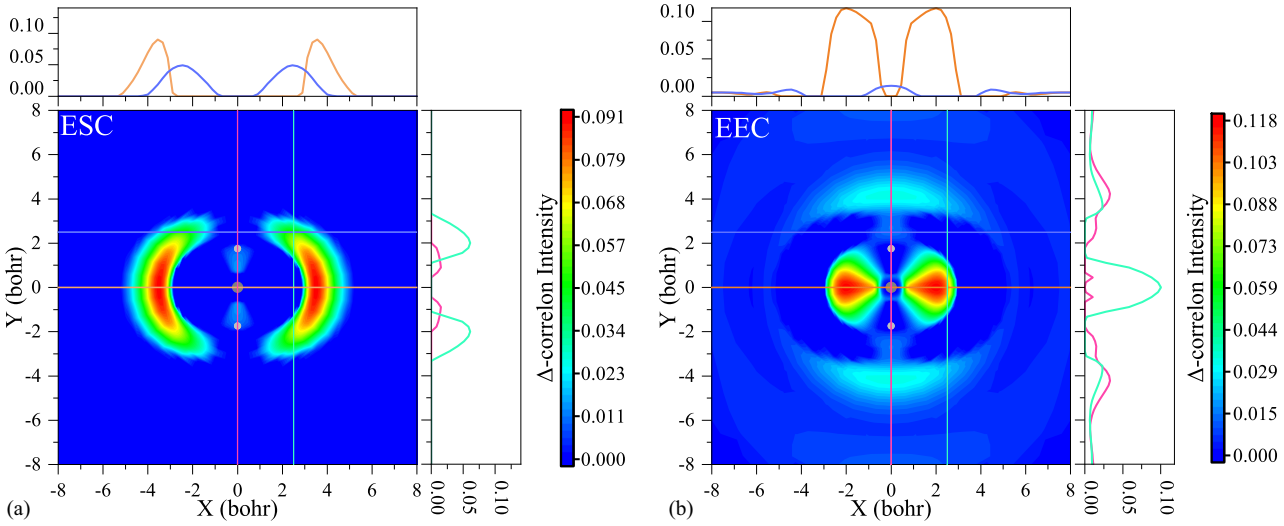

FIG. 5. Plots of ESC (left panel) and EEC (right panel) Δ-correlon functions, cf. Eqs. (16) and (17), respectively, for the $\Pi_u(\pi \to 3s)$ state of C_2H_4. The XY plane is perpendicular to the axis of the molecule and includes the position of one of the C nuclei located in the center.

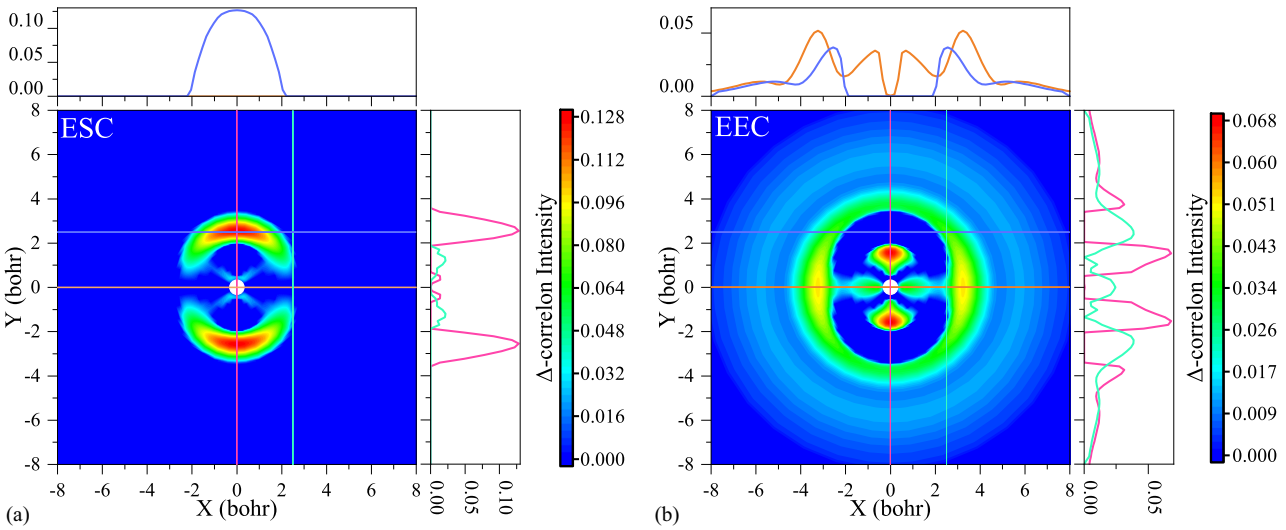

FIG. 6. Plots of ESC (left panel) and EEC (right panel) Δ-correlon functions, cf. Eqs. (16) and (17), respectively, for the $\Pi_u(\pi \to 3s)$ state of N_2. The XY plane is perpendicular to the axis of the molecule and includes the position of one of the N nuclei located in the center.

$\Sigma_u^-(\sigma \to \sigma^*)$ state of H_2 obtained with the CAS(2,32) in the cc-pVTZ basis. The plots are made in the plane passing through the H–H bond.

One can see from Fig. 7(b) that the EEC Δ-correlon wins the whole interior of the H–H bond including that in the vicinity of the H nuclei. And the ESC Δ-correlon is pushed to the outer region, though it includes also the positions in the outer vicinity of the H nuclei [see Fig. 7(a)]. In order to provide the explanation for this reversal, we use the two-determinantal two-electron model of Sec. III, which is even more realistic for the two-electron H_2 molecule. Specifically, we consider the analytical expressions of this model at the midpoint $\boldsymbol{r}_{bm}$ of the bond A–B.

First of all, we note that the excited state function $X_e^{\rm act}(\boldsymbol{r})$ of Eq. (22) has the node at $\boldsymbol{r}_{bm}$, where $\chi_a(\boldsymbol{r}_{bm}) = \chi_b(\boldsymbol{r}_{bm})$, i.e.,

$$X_e^{\rm act}(\boldsymbol{r}_{bm}) = 0. \tag{31}$$

On the other hand, with $\chi_a(\boldsymbol{r}_{bm}) = \chi_b(\boldsymbol{r}_{bm})$ and $c_2^2 = 1 - c_1^2$, one finds that the ground-state function $X_g^{\rm act}(\boldsymbol{r}_{bm})$ of (26) exceeds 1,

$$X_g^{\rm act}(\boldsymbol{r}_{bm}) = \frac{1}{c_1^2} > 1, \tag{32}$$

which is the signature of anticorrelation squeezing. This shows that the latter is not the exclusive characteristic of the valence ionic excitation in the minimal model. Rather, anticorrelation squeezing also emerges locally (around $\boldsymbol{r}_{bm}$) for the ground state.

The difference between Eqs. (31) and (32) is negative, which means that the region around $\boldsymbol{r}_{bm}$ is occupied with the EEC Δ-correlon. Since the H–H bond is exceptionally short and the hydrogenic atomic orbitals are relatively diffuse, the estimates Eqs. (31) and (32) are valid for the whole interior

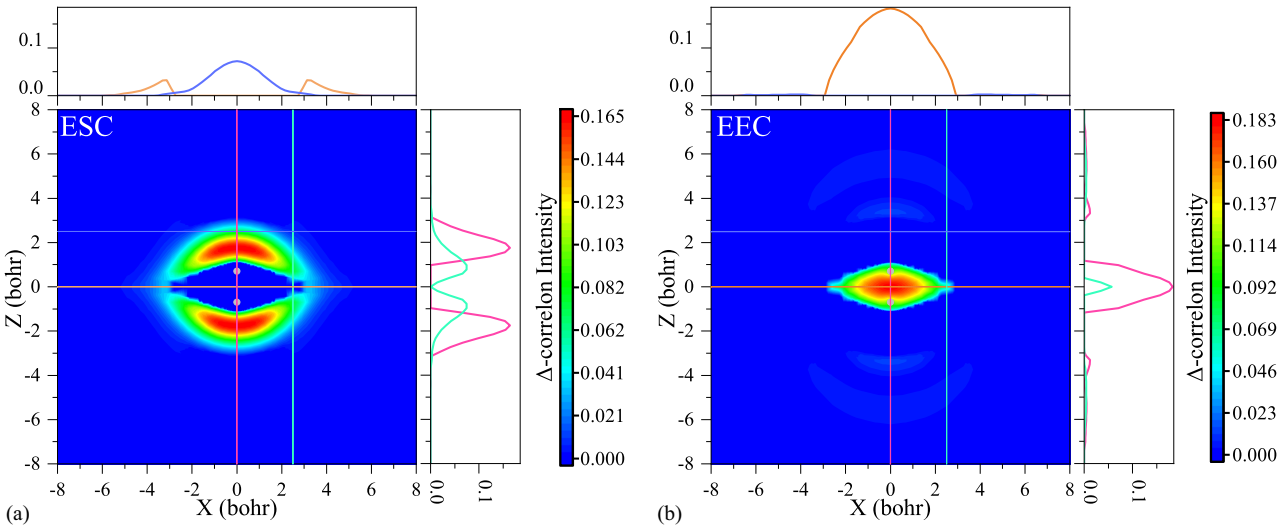

FIG. 7. Plots of ESC (left panel) and EEC (right panel) Δ-correlon functions, cf. Eqs. (16) and (17), respectively, for the $\Sigma_u^-(\sigma \to \sigma^*)$ state of H_2. The Z plane passes through both H nuclei.

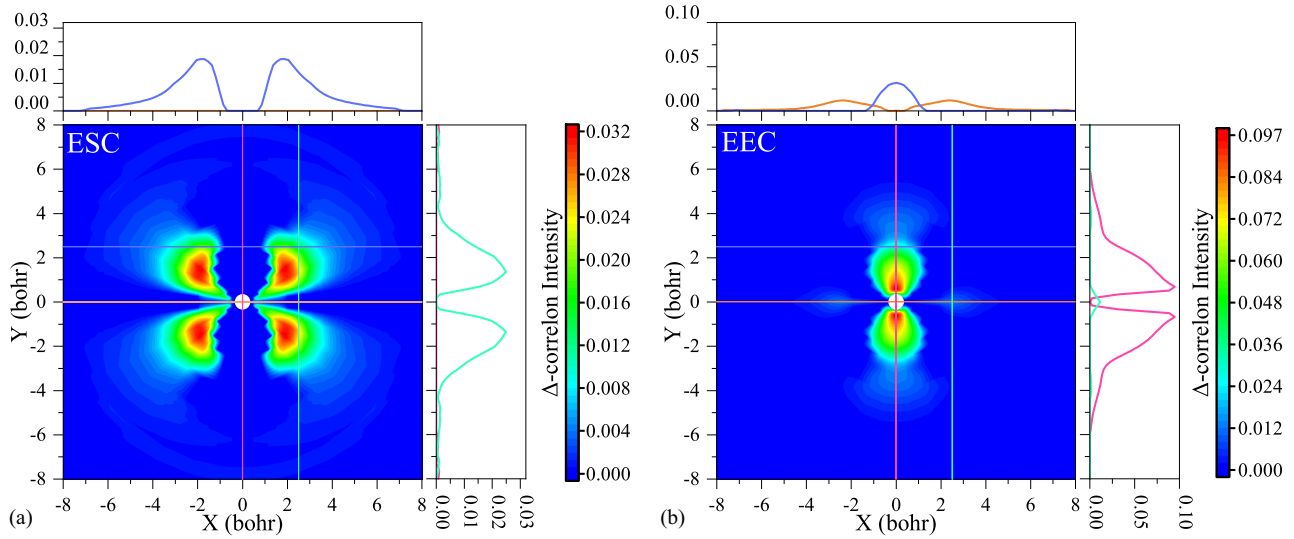

FIG. 8. Plots of ESC (left panel) and EEC (right panel) Δ-correlon functions, cf. Eqs. (16) and (17), respectively, for the $\Pi_g(\sigma \rightarrow \pi^*)$ state of N_2. The XY plane is perpendicular to the axis of the molecule and includes the position of one of the N nuclei located in the center. CAS(2,2) wave function used.

of the H–H bond. This explains the observed behavior of the EEC Δ-correlon for the $\Sigma_u^-(\sigma \rightarrow \sigma^*)$ state of H_2.

Another special case is the $\sigma \rightarrow \pi^*$ excitation in the N_2, the analog of which for the C_2H_4 was considered in Sec. IV A. Figures 8–10 provide the example of the definite qualitative changes in the behavior of the ESC and EEC Δ-correlons with the level of electron correlation included.

Indeed, at the minimally correlated CAS(2,2) level the EEC Δ-correlon wins the energetically favorable positions, forming a sizable p shape in the vicinity of the N nucleus [see Fig. 8(b)]. As opposed to this, the ESC Δ-correlon is pushed outwards, forming a halo around the EEC Δ-correlon [see Fig. 8(a)]. Then, at the higher CAS(4,8) level the ESC Δ-correlon moves closer to the N nucleus [see Fig. 9(a)]. As the result, the Δ-correlons occupy the regions along the different axes in the plane of the plot [see Fig. 9(b)]. Finally, at the highest CAS(6,20) level, the ESC Δ-correlon moves still closer to the N nucleus, localizing in two ellipse-shape regions at one of the axis [see Fig. 10(a)]. In turn, the EEC Δ-correlon forms a small p-shape along another axis as well as a halo around the ESC Δ-correlon [see Fig. 10(b)].

The specific feature of the considered excitation is that the σ and π^* MOs of N_2 are rather localized (more than the analogous MOs of C_2H_4) on the different bonds of N_2. Then, their relatively low overlap produces the lowering of the corresponding on-top functions due to enhanced-correlation spreading akin to that for the Rydberg excitations considered

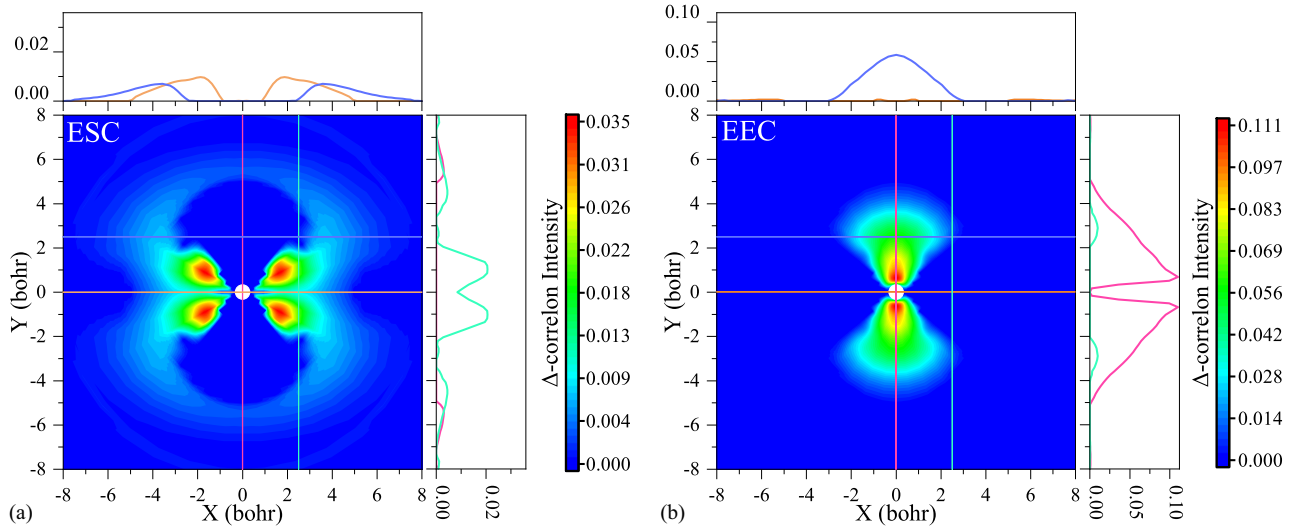

FIG. 9. Plots of ESC (left panel) and EEC (right panel) Δ-correlon functions, cf. Eqs. (16) and (17), respectively, for the $\Pi_g(\sigma \rightarrow \pi^*)$ state of N_2. The XY plane is perpendicular to the axis of the molecule and includes the position of one of the N nuclei located in the center. CAS(4,8) wave function used.

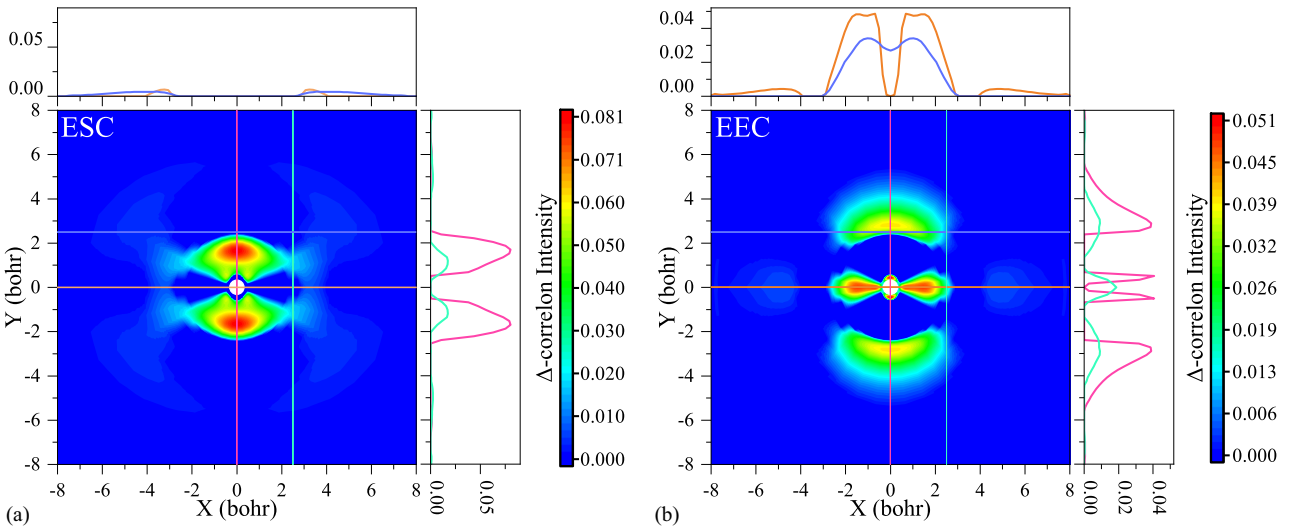

FIG. 10. Plots of ESC (left panel) and EEC (right panel) Δ-correlon functions, cf. Eqs. (16) and (17), respectively, for the $\Pi_g(\sigma \rightarrow \pi^*)$ state of N_2. The XY plane is perpendicular to the axis of the molecule and includes the position of one of the N nuclei located in the center. CAS(6,20) wave function used.

in Sec. IV B. Apparently, at the lowest correlated CAS(2,2) level a combination of this enhanced-correlation spreading with anticorrelation squeezing is stronger than the genuine electron correlation in the ground state. This determines a favorable energetically position of the EEC Δ-correlon at this level mentioned above.

It appears, however, that the additional correlation included at the higher CASSCF levels is consistently larger in the ground state compared to that in the excited state. This explains an increasingly more competitive behavior of the ESC Δ-correlon in comparison with EEC Δ-correlon depicted in Figs. 9 and 10.

V. CONCLUSIONS

The Δ-correlon quasiparticles proposed in this paper offer a condensed description of the interplay of two, arguably, most interesting electron effects, electron correlation and electron excitation. The quasi-one-particle description of the former effect is achieved by considering the pair-correlation functions at the special coalescence points of the configurational space. Then, the comparison of such a correlation for a given excited and the ground state within the Δ-correlon wave function provides the condensed description of the excitation effect on electron correlation. The complex form of the Δ-correlon wave function allows us to naturally separate the regions with the excitation suppression of correlation (ESC Δ-correlon), where correlation is stronger in the ground state, from those with the excitation enhancement of correlation (EEC Δ-correlon), where correlation is stronger in the excited state.

Application of the proposed Δ-correlon approach to the description of the important single excitations allows us to meaningfully compare correlation in singly excited states with the canonical correlation in the ground state which is, mainly, partially doubly excited reference determinant. The notion of the effective correlation in single excitations is introduced with the competition of anticorrelation squeezing and enhanced-correlation spreading. The former effect characterizes single valence excitations of the ionic nature and this leads to the prevailing of the ESC effect in this type of excitations. Enhanced-correlation spreading characterizes, on the other hand, single Rydberg excitations, which leads to the prevailing of the EEC effect.

The proposed Δ-correlon quasiparticles are studied both analytically and numerically. The analytical expressions for the on-top correlation functions are obtained with the two-electron two-orbital model of the active space of an excitation. The 2D contour plots of the ESC and EEC Δ-correlons obtained for the lowest vertical valence ionic and Rydberg excitations in the prototype molecules H_2, N_2, and C_2H_4 from the highly correlated wave functions confirm, in general, the trends in the relative correlation strength deduced from the model. This indicates that, unlike the covalent and ionic correlons of our previous work [1], the present concept of Δ-correlons is robust not only at the multiconfigurational (MCSCF) level with a restricted account of correlation, but also at the highly correlated level of many-electron theory.

ACKNOWLEDGMENTS

This work was supported by the Narodowe Centrum Nauki of Poland under Grant No. 2017/27/B/ST4/00756.

[1] M. R. Jangrouei, K. Pernal, and O. V. Gritsenko, Phys. Rev. A **102**, 052829 (2020).
[2] R. S. Knox, *Theory of Excitons* (Academic, New York, 1963).
[3] J. Frenkel, Phys. Rev. **37**, 17 (1931).

[4] G. H. Wannier, Phys. Rev. **52**, 191 (1937).
[5] A. D. Becke, A. Savin, and H. Stoll, Theor. Chim. Acta **91**, 147 (1995).
[6] A. Szabo and N. S. Ostlund, *Modern Quantum Chemistry: Introduction to Advanced Electronic Structure Theory* (Dover, Mineola, NY, 1989).
[7] P. Hohenberg and W. Kohn, Phys. Rev. **136**, B864 (1964).
[8] W. Kohn and L. J. Sham, Phys. Rev. **140**, A1133 (1965).
[9] R. G. Parr and W. Yang, *Density-Functional Theory of Atoms and Molecules* (Oxford University Press, New York, 1989).
[10] R. M. Dreizler and E. K. U. Gross, *Density Functional Theory: An Approach to the Quantum Many-Body Problem* (Springer, Berlin, 1990).
[11] E. Fromager, J. Toulouse, and H. J. Jensen, J. Chem. Phys. **126**, 074111 (2007).
[12] G. Li Manni, R. K. Carlson, S. Luo, D. Ma, J. Olsen, D. G. Truhlar, and L. Gagliardi, J. Chem. Theory Comput. **10**, 3669 (2014).
[13] E. Hedegard, S. Knecht, J. S. Kielberg, H. J. Jensen, and M. Reiher, J. Chem. Phys. **142**, 224108 (2015).
[14] O. V. Gritsenko, R. van Meer, and K. Pernal, Phys. Rev. A **98**, 062510 (2018).
[15] A. Ferté, E. Giner, and J. Toulouse, J. Chem. Phys. **150**, 084103 (2019).
[16] M. Hapka, K. Pernal, and O. V. Gritsenko, J. Chem. Phys. **152**, 204118 (2020).
[17] M. Hapka, K. Pernal, and O. V. Gritsenko, J. Phys. Chem. Lett. **11**, 5883 (2020).
[18] N. C. Handy and A. J. Cohen, Mol. Phys. **99**, 403 (2001).
[19] R. Colle and O. Salvetti, J. Chem. Phys. **93**, 534 (1990).
[20] P. Gori-Giorgi and A. Savin, Phys. Rev. A **73**, 032506 (2006).
[21] O. V. Gritsenko, R. van Meer, and K. Pernal, Chem. Phys. Lett. **716**, 227 (2019).
[22] O. V. Gritsenko and K. Pernal, J. Chem. Phys. **151**, 024111 (2019).
[23] K. Pernal, O. V. Gritsenko, and R. van Meer, J. Chem. Phys. **151**, 164122 (2019).
[24] K. Pernal and O. V. Gritsenko, Faraday Discuss. **224**, 333 (2020).
[25] C. Lee, W. Yang, and R. G. Parr, Phys. Rev. B **37**, 785 (1988).
[26] S. S. Shaik and P. C. Hiberty, *A Brief Tour through Some Valence Bond Outputs and Terminology* (John Wiley & Sons, New York, 2007), Chap. 2, pp. 26–39.
[27] C. Angeli, J. Comput. Chem. **30**, 1319 (2009).
[28] T. H. Dunning Jr., J. Chem. Phys. **90**, 1007 (1989).
[29] R. A. Kendall and T. H. Dunning Jr., J. Chem. Phys. **96**, 6796 (1992).